Eur. Phys. J. B (2019) 92: 28
https://doi.org/10.1140/epjb/e2018-90562-1

THE EUROPEAN PHYSICAL JOURNAL B

Regular Article

Multi stability and global bifurcations in epidemic model with distributed delay SIRnS-model

Gorm Gruner Jensen[1,a], Florian Uekermann[2], and Kim Sneppen[2]

[1] Institute for Theoretical Physics, University of Bremen, Hochschulring 18, 28359 Bremen, Germany
[2] Niels Bohr Institute, University of Copenhagen, Blegdamsvej 17, 2100 Copenhagen, Denmark

Received 21 September 2018 / Received in final form 27 November 2018
Published online 6 February 2019

Abstract. Many diseases, such as influenza and the common cold, cause recurrent epidemics. The classical SIRS model fails to obtain recurrent epidemics as it predicts a globally stable endemic fixed point. This endemic fixed point is, however, linearly unstable for most parameters, if one assumes that the time spent in the recovered state is deterministic rather than exponentially distributed. In that case all trajectories converge to a stable epidemic limit cycle. It has been shown that a similar region of instability exists for systems with intermediate immune time distributions. Furthermore, it has been suggested that a bistable region could exist. Here, we first characterize this bistable region using a combination of direct simulation and bifurcation theory. We find that it has a bound where the stable epidemic limit cycle annihilates with an unstable limit cycle in a non-local bifurcation. Secondly, we extend the bifurcation-analysis to narrower immune time distributions than previous studies. Here, we find new levels of complexity in the bifurcation diagram, including the possibility for at least two different epidemic limit cycles at the same disease parameters. Overall our study highlights that a given disease may have multiple epidemic signatures, dependent on how it is introduced.

1 Introduction

Models of spreading of infectious diseases [1–3] are an integrated and important element in the analysis of epidemics. Typically such models are variations of the so called SIR-models [1]; describing a population of hosts who can each be in one of the three states Susceptible, Infectious, or Recovered. For a number of diseases, like most respiratory viral infections, the immunity following infections is neither complete nor permanent. This is modeled by allowing hosts to escape from the recovered (or immune) R-state and back to the susceptible S-state. It has been shown that in the simplest case, when the infection-rate is linear with the number of infectious host and the other transitions happen with constant rate, the thereby defined SIRS model has two fixed-points, one endemic and one disease-free, and that one will always be globally stable [4]. This is in disagreement with the observation of periodic epidemic out-breaks of for example influenza. A number of mechanisms have been proposed to reproduce the observation of repeated epidemic oscillations. These include time dependent, oscillating parameters [5,6], non-linear infection rates [7], infection networks [8–11], finite population noise [12,13], and narrow transition-time distributions [14–18]. This paper focus on the latter, by analyzing the SIRnS-model originally proposed by Hethcote et al. [19] (Fig. 1). In this model the narrow immune-time distribution is achieved by replacing the R-state with a sequence of n states, each with constant transition-rates. The advantage of this approach is that the variance of the distribution can be easily varied – as it goes as $1/n$ – while still using only ordinary differential equations.

Previous examinations of the model have focused on fixed-points and their stability [19,20], and local bifurcation theory has been used to demonstrate the existence of limit-cycles [19]. Here we extend these investigations by direct numerical integration, which allows us to learn more about the periodic solutions than their mere existence.

In particular, we investigate the shape of the parameter region where there exist multiple metastable states – a stable limit-cycle and a stable endemic fixed-point. This was proposed in Hethcote et al. [19] but not quantitatively analyzed. Further, when extending our analysis to much narrower immunity-time distributions we discover an increasingly complex structure of the local bifurcation-scheme for the endemic fixed-point. Accordingly, we find that the same disease can exhibit different types of epidemic behavior dependent on initial conditions. This existence of multiple alternate limit-cycles, may be graphically interpreted as 'epidemic overtones'.

[a] e-mail: ggjensen@itp.uni-bremen.de

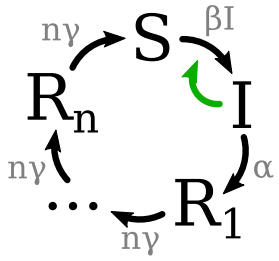

Fig. 1. Schematic description of the SIRnS-model. The total duration of the removed (immune state) is $\tau = 1/\gamma$ is split into n substates. The black arrows represent the state transitions of individual agents. The green arrow indicates that the transition $S \to I$ happens with a rate that is proportional to the number of infected hosts (I).

2 Model

We consider spreading of diseases in a well mixed population of hosts that each can be Susceptible, Infectious or Resistant. Further, we assume that hosts can change cyclically between the states, $S \to I \to R \to S$ and thus again become susceptible after some period in the resistant state. The transition $S \to I$ occurs with a rate proportional to the infectious fraction of the population, I, and the transition $I \to R$ happens with constant rate. Our objective is to analyze how the epidemic pattern behavior depends on the probability-distribution of the time spent in the resistant state. As was already discussed by Hethcote et al. [19], there is a class of time-distributions which can be rephrased into ordinary differential equations, namely the ones that can be reproduced by a chain of n sub-steps:

$$\frac{dS}{dt} = -\beta \cdot I \cdot S + n\gamma R_n \tag{1}$$

$$\frac{dI}{dt} = \beta \cdot I \cdot S - \alpha \cdot I \tag{2}$$

$$\frac{dR_1}{dt} = \alpha \cdot I - n\gamma R_1 \tag{3}$$

$$\frac{dR_i}{dt} = n\gamma R_{i-1} - n\gamma R_i \quad \text{for} \quad i = 2, 3, \ldots, n \tag{4}$$

$$1 = S + I + \sum_{i=1}^{n} R_i. \tag{5}$$

The average time a host spends in the infectious state is $1/\alpha$. In the following we will use this as the time-unit by setting $\alpha = 1$.

We call this the SIRnS model. For $n = 1$ the distribution of immune times for individual hosts is exponential. Thus in an agent based implementation of the $n = 1$ model, each individual will switch from resistant to susceptible state at a time t that is distributed as $P(t) = \gamma \exp(-\gamma t)$. This is unrealistic since it implies that individuals can loose the gained immunity/resistance immediately after recovering after they have recovered from the infection. The distribution of the time it takes to pass through a chain of n states, each with a constant transition-rate $n\gamma$, is obtained by calculating the n-fold convolution of exponential distributions:

$$P(t) = \frac{(n \cdot \gamma \cdot t \cdot e^{-\gamma t})^n}{t \cdot (n-1)!}, \tag{6}$$

which has the mean value $\langle t \rangle = \tau = \frac{1}{\gamma}$ (independent of the number of states) and the standard-deviation $\sigma_t = \frac{1}{\gamma\sqrt{n}} = \frac{\tau}{\sqrt{n}}$. From this we see that splitting the removed state into a longer chain, results in a more narrow time distribution. In the limit $n \to \infty$ the distribution will converge to a delta-distribution, corresponding to a deterministic delay. In this case the model reduces to a set of delay differential equations that have been extensively studied before [7,15,16,21].

The basic reproduction number for the disease, $R_0 = \beta/\alpha$, quantifies the capacity of the disease to spread in a completely susceptible population. From equation (2) it is easy to see, that if $R_0 < 1$ then the growth rate of the fraction of infectious hosts is negative even in a completely susceptible population $S = 1$. Hence our analysis will only be of interest for $R_0 > 1$, corresponding to cases for which either repeated epidemics or an endemic state are possible. As we will see later, rich epidemic behavior is only possible if R_0 is not too large, i.e. alternative states of epidemic dynamics are only seen for moderate R_0 values.

2.1 Parameter summary

The above set of equations can be fully characterized by 3 parameters, the basic reproduction number $R_0 = \beta/\alpha$, the average duration of the resistant state $\tau = 1/\gamma$, and the number of states in the resistant state chain n, which determines the width of the duration distribution.

3 Methods

This paper presents a sequence of results concerning the coexistence of linearly stable attractors in the SIRnS-model.

First we use a Gillespie simulation to illustrate how finite system noise can result in stochastic switching between metastable attractors (Fig. 2). In this case the two attractors are an endemic fixed point and an epidemic limit-cycle.

The main part of the results, however, are about the deterministic system arising in the thermodynamic limit of infinitely many hosts. As long as the basic reproduction number, R_0, is greater than one, this system always has a single endemic fixed-point, which can be calculated analytically [19]. The stability of this fixed-point can be determined by the linearizing the dynamics around it, and inspecting the eigenvalues of the corresponding matrix. When any of these eigenvalues has a real part greater than zero, the fixed-point in unstable. The linear stability results presented in this paper are found by first calculating the matrix of the linearized dynamics analytically, following the same procedure presented by Hethcote et al. [19], and then numerically calculating its eigenvalues point-wise (in parameter space).

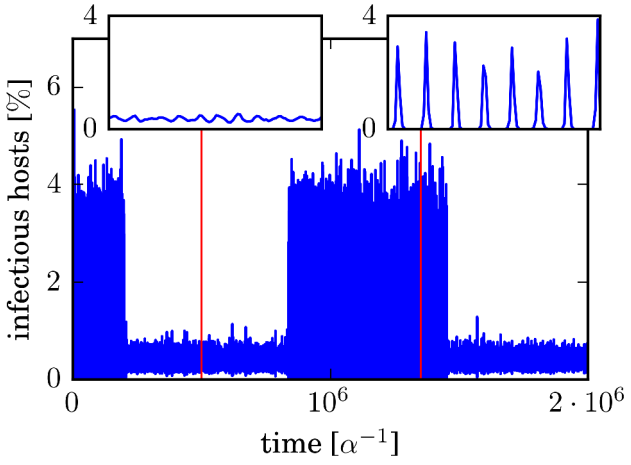

Fig. 2. The SIRnS-model can exhibit bi-stability and can then switch between alternate attractors of epidemic behaviour. This is here demonstrated in an agent based model with 1 million hosts, $n = 9$, $\alpha = 1$, $\beta = 1.6$ and $\gamma = 1/100$. The update is done by a Gillespie type algorithm [22] in which each agent i is assigned a time for next transition $\Delta t_i = -\ln(rand_i)/rate_i$ with $rate_i$ as the corresponding transition rate from equations (1)–(4) and $rand_i \in [0, 1)$ is drawn from a uniform random distribution. The first update is chosen, and procedure repeated. To prevent extinction, a small external source of infection is added, corresponding to one constantly infectious host. The figure shows percentage of infectious hosts as a function of time. The inserts show examples of the behaviour at each of the attractors.

In order to investigate the non-local bifurcations, we rely on numerical integration of the differential equations using the Euler method. In general the stable endemic limit-cycle with the largest amplitude is the attractor reached by the dynamics when initializing the system in a state where the entire population is infectious. This is the method behind the parameter-scan shown in Figure 3, where such a simulation is performed for each pixel.

In the case where we both detect a stable endemic limit-cycle and the local linear stability analysis show that the endemic fixed-point is stable, we search for an unstable limit-cycle using the following approach: first we analytically calculate the endemic fixed point, x_0, and choose any point, x_1, which is located on the epidemic limit cycle. We then initiate the system at different points on a straight line between the x_0 and x_1, defined by $(1 - a) \cdot x_0 + a \cdot x_1$ with $a \in (0, 1)$. We use bisection to search for a critical value, a^*, such that trajectories starting at points with $a < a^*$ will converge to the endemic fixed-point, while those with $a > a^*$ converge to the epidemic limit-cycle. When trajectories are initiated very close the critical point, we observe extremely long transients. The major part of such a transient is spent in an almost periodic (but unstable) orbit. We plot these transient trajectories as *the unstable limit-cycle* when we have found initial-conditions close enough to the critical point, that they can complete multiple epidemic outbreaks (orbits) with variations small enough to be invisible to the human eye.

In some cases the local linear stability-analysis indicates the coexistence of two stable epidemic limit-cycles. If the endemic fixed-point is unstable, the limit-cycle with the smallest amplitude can be found as the attractor of trajectories initiated very closed to that. To find the small stable limit-cycles for parameters where the endemic fixed-point is linearly stable (such as in Fig. 4c) we first find the small limit-cycle for a near-by parameter point where the endemic fixed-point is unstable, and then continue running the dynamics while slowly changing the parameters to the desired point.

For the numerical integrations we have chosen the simplest possible option, namely the Euler-method. This method is sometimes criticized for its poor error propagation properties which may cause instability, especially in marginally stable systems. For linearly stable trajectories, however, the dynamics are automatically correcting errors as long as they are small enough to stay within the basin of attraction. Therefore we have prioritized simplicity over better error convergence rates.

All figures are produced using a timestep of $\Delta t = 0.001$ (in units of the mean susceptibility time). To verify that this choice is small enough, we have compared some our results with simulations with both smaller and larger timesteps. We find that the orbits are indistinguishable by visual inspection when the timesteps are a factor ten smaller, and that the qualitative behaviors are robust even when the timesteps are a factor ten larger.

4 Results

First let us consider the SIRnS model with a typical set of realistic parameters. We choose a transmission rate characterized by $R_0 = 1.6$ and a resistance period $\tau = 100$ with a relative spread between individuals of one third ($n = 9$). Such conditions may lead to both endemic and epidemic behaviour. Thus both behaviours can be seen with the same set of parameters (n, R_0, and γ). As Figure 2 illustrates, the noise introduced by simulating a finite population size (1 million hosts) allows for transitions between a linearly stable epidemic limit-cycle and a linearly stable endemic fixed-point. Below we present a systematic analysis of alternating dynamical behaviour in the SIRnS model as the parameters are varied.

For $n \in \{1, 2\}$ and $R_0 > 1$ it can be been shown that the endemic fixed-point is globally stable [23,24].

When $n \geq 3$ the parameter space has a region of linear instability of the endemic fixed-point as described by [19]. As long as n is relatively small, this region of instability corresponds to one pair of eigenvalues, of the linearized dynamics matrix (expanded around the endemic fixed-point), having a positive real part. The bifurcation scheme is indicated in Figure 3 in the case of $n = 9$ (corresponding to a relative standard deviation of 1/3 of the time spend in the recovered state chain): the dashed black line indicate the local bifurcation of the endemic fixed-point, and bounds the region of linear instability. Consider a gradual increase of R_0 for a given high value of $\tau >> 1$. For R_0 that slightly exceeds 1, the endemic fixed point becomes unstable. At this transition a stable limit cycle

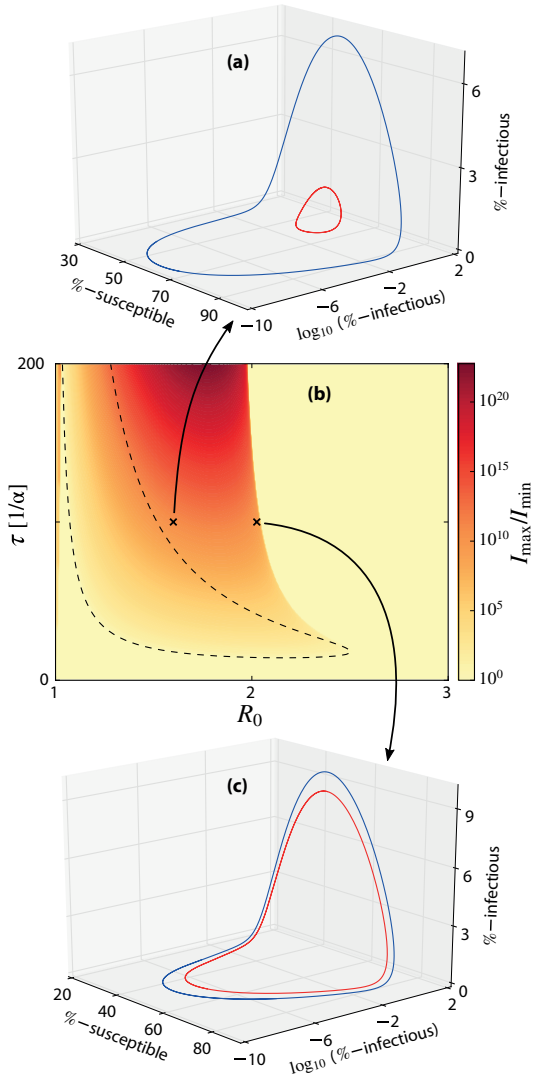

Fig. 3. (b) Parameter scan of maximum to minimum ratio of infected hosts, during epidemic cycles epidemic cycle. The black, dashed line encloses a region where the endemic fixed-point is linearly unstable, see also [19]. The black crosses mark the parameters for the top and bottom figure. The parameter-scan is performed in an SIRnS-model with $n = 9$ resistant states. (a) and (c) Stable epidemic limit-cycle [blue, outer] and the unstable limit-cycle [red, inner] at parameters marked in the middle-figure ($R_0 = 1.6$ in (a) and $R_0 = 2.025$ in (c); $\tau = 100$ in both). Notice I is shown on one axis whereas $\log_{10}(I)$ is shown on another axis. This allows us to track the dynamics at extremely low values of I.

corresponding to recurrent epidemics emerges, shown as the blue (outer) orbit in Figures 3a and 3c. At higher R_0 (~ 1.5) the endemic fixed-point becomes stable again, by emitting an unstable limit-cycle. This unstable limit cycle, shown as the red (inner) curve in Figures 3a and 3c, separates two alternative types of dynamics of the disease. Accordingly, a bistable regime of the SIRnS-model occurs when the endemic fixed-point undergoes a sub-critical Hopf-bifurcation, 'emitting an unstable limit-cycle'. This bi-stability was suggested in [19], but no explicit orbits were shown. Increasing the value of R_0 further to about ~ 2, the stable endemic limit-cycle "merges and annihilates" with the unstable limit-cycle in a global bifurcation. This is indicated in panel (c) where the inner (red) orbit is close to the outer (blue) one. For R_0 greater than critical value at which the two limit-cycles annihilate, the stable endemic fixed-point appears to be the only attractor of the system. A similar bifurcation scheme is observed in a related cellular automaton representing a discrete time version of the SIRnS model [25]. In between these two R_0 values, the model has two attractors and can exhibit the bi-stable switching shown in Figure 2 if simulated with random infections and recovery in a finite population. In practice, one of these attractors might have a much longer escape-time than the other and it may therefore be difficult to observe both states in a given historical record.

It is worth noting that for the epidemic limit-cycles, the fraction of infectious hosts tend to get very low between the epidemic outbreaks, especially when the immune-times are long and narrowly distributed.

Since the maximal fraction of infectious hosts during one period, $I_{\max}$, is smaller than one it follows from the parameter scan in Figure 3b that the minimal fraction, $I_{\min}$, falls below 10^{-20} as the average immune-time approaches 200 infectious periods (distributed on 9 immune states, and with an R_0-value around 1.8). Such a low infection-level would clearly mean extinction of the disease in any realistic human population. Even for much shorter average immune-times, $I_{\min}$ become so small that the disease would be very susceptible stochastic fluctuations in a finite population. To circumvent this problem in the finite population simulation shown in Figure 2 we have had to introduce a small external source of infection, corresponding to one eternally infectious host.

The bifurcations scheme in the SIRnS model becomes more complex, when the distribution of immune times becomes even narrower ($n \gtrsim 20$). The small variance allow for a new mode of stable limit cycles, in which the epidemic outbursts are smaller, but more frequent. Consequently, it becomes possible for one given disease to express different periodically epidemic patters without a change in parameters. For example, one set of initial conditions could lead to an epidemic every year, whereas another starting condition could lead to returning epidemics every third year.

An example of two different epidemic signatures with the same parameters is illustrated in Figure 4. In Figure 4a the region of instability is shown in orange. This region consists of two distinct patches. As in the previous $n = 9$ case (Fig. 3), the presence of each patch signals the onset of epidemic limit cycle that in fact survives also to values of R_0 that are larger than the orange region indicates. Figures 4b and 4c show two different limit cycles which are obtained at the same parameter point $R_0 = 1.8$ and $\tau = 250$. This parameter point is marked by the red dot in Figure 4a, from which it is clear, that the endemic fixed point is also linearly stable. Consequently this disease actually has three stable attractors. One endemic fixed-point, and two different epidemic limit cycles.

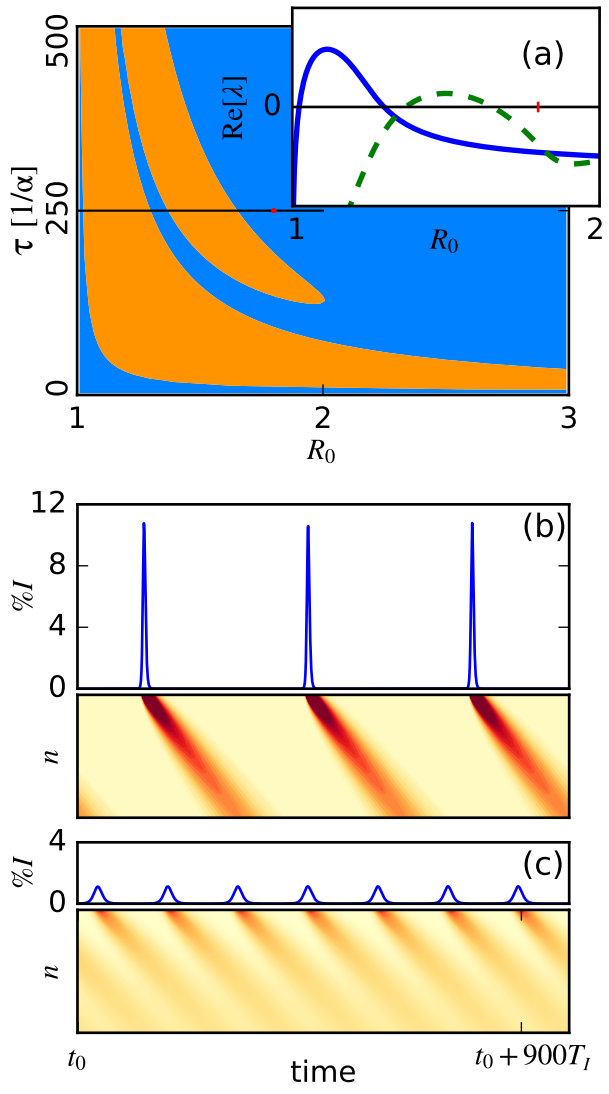

Fig. 4. (a) The orange region mark parameters for which the endemic fixed-point in SIRnS-model with $n = 25$ is unstable. The inset shows the two largest real parts of (non-trivial) eigenvalues of the linear stability analysis as a function of R_0, for $\tau = 250$. The two 'tongues of instability' observed in the main panel correspond to different eigenvalue-pairs, and thereby to different types of epidemic patterns. The red dot at $R_0 = 1.8$ and $\tau = 250$ mark the parameter-set used to obtain the time series in both panel (b) and (c). (b) Dynamics of epidemic limit-cycle reached from an initial condition with a fully infectious population. (c) Dynamics of epidemic limit-cycle at the 'second tongue of instability' (highest value of R_0). In (b) and (c) the vertical axis in the lower panels index the resistant states with R_1 at the top to R_{25} at the bottom. The hosts is distributed as indicated by the intensity of red.

The inset in Figure 4a shows the two largest real parts of (non-trivial) eigenvalues of the linearized dynamics matrix as a function of R_0, for constant average immunity-period $\tau = 250$. This illustrates that the two orange patches correspond to two different pairs of eigenvalues having positive real part.

The bottom part of these panels indicates the fraction of the population in each of the 25 removed states

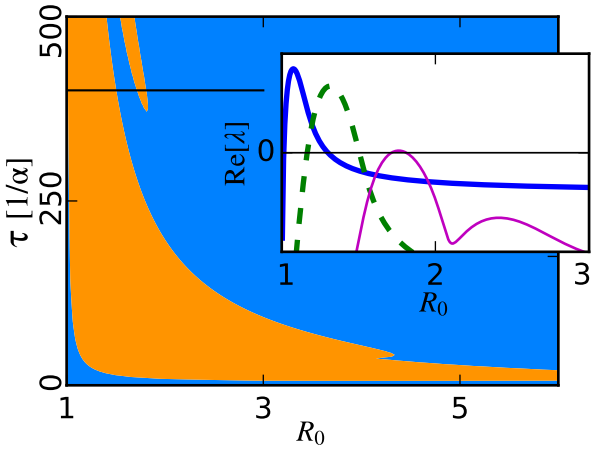

Fig. 5. This figure uses same color scheme as the top-panel in Figure 4, but shows the results of $n = 49$ resistant states. The orange unstable area now consist of three patches corresponding to three different eigenvalue-pairs. Two of the patches have a substantial overlap (R_0 values where blue and dashed blue curves both are above zero in the inset). The eigenvalues shown in the inset are calculated at $\tau = 400$, as indicated by the horisontal black line in the main figure.

(listed from top to bottom). In Figure 4b almost the entire population is infected during an epidemic outbreak. The population then 'moves as a slowly dispersing wave across the string of removed states', and accumulate in the susceptible state (not plotted), waiting for the next epidemic outbreak to occur. In Figure 4c a smaller fraction of the population is infected per epidemic outbreak and therefore a new outbreak can begin even before the bulk of the wave of the previous infections has reached the susceptible state. As a consequence, 'the string of susceptible states' now simultaneously carries two waves as a kind of 'epidemic overtone'.

We have found that new patches of linear instability of the endemic fixed-point keep occurring, as n increases, and the duration of the resistant states becomes increasingly deterministic. Figure 5 shows the more exotic region of linear instability of the endemic fixed point for $n = 49$ (relative standard deviation of 1/7). The region is now composed of three patches, corresponding to each their pair of eigenvalues. The inset shows the real parts of the corresponding three eigenvalues as a function of R_0, for a fixed average resistance period of $\tau = 400$.

The 'first' and 'second' patch overlap. Hence there is no Hopf-bifurcation at the lower (in terms of R_0) boundary of the second patch, and no stable limit-cycle is emitted. A full understanding of this bifurcation-scheme will require further investigation.

The third patch has no overlap with the two others, and investigations similar to those shown in Figure 3 confirm that, for increasing R_0 across this patch, first a stable endemic limit-cycle is emitted, then an unstable limit-cycle, and finally the two 'collide and annihilate'. Thus for $n = 49$ we also find a maximum coexistence of three linearly stable attractors.

5 Discussion

The simple disease spreading models started by the classical work of Kermack [1] had a decisive impact on our way to characterize and predict epidemics in our society. By considering that resistant or removed hosts may re-enter the population as susceptible individuals, this kind of 'mass-action' kinetics has let to insights into recurrent epidemics as well. However, the details of how this reintroduction happens matters. In some cases, the disease mutates and the new epidemic of the mutant will be influenced by mutation rates and possible random properties associated to genomic variants.

In other cases, recurrent epidemics are remarkably periodic suggesting simpler models with relatively deterministic re-population of the fully susceptible population. The SIRnS model analyzed here addresses the latter scenario.

Previous investigations of immune time distributions mainly approached the problem using integro differential equations. This method allows investigations of arbitrary distributions of immunity times. And as Gonçalves et al. point out [20]: "An accurate model should implement the distributions based on empirical data". However, there is very little available knowledge on distributions of immune times. In this light, the chain of constant-rate processes in the SIRnS model provides a simple way to represent a family of increasingly narrow distributions immune times.

One new finding is that a finite variance of the immunity-time distribution results in a finite upper bound for R_0 above which the endemic fixed point is the only attractor. This bound seems to increase as the variance goes to zero, which is in agreement with previous studies showing that the endemic fixed-point stays unstable for arbitrarily large R_0 in the deterministic case [20]. Our simulations strongly suggest, that this transition is a global bifurcation in which the stable epidemic limit-cycles vanishes by 'collision and annihilation' with a corresponding unstable limit-cycle.

We have shown that for intermediate width of the duration of the resistant/immune state, at least two stable limit-cycles can coexist. These attractors may be interpreted as epidemic overtones. Finally, we have shown that such 'overtones' may become unstable as the immune time distribution becomes increasingly deterministic, which is in agreement with previous studies of the fully deterministic case, which have reported no such overtones. Noticeably Abramson et al. [26] consider the deterministic delay limit with a seasonal variation of R_0. At some driving frequencies they found complex chaotic attractors that could be interpreted as an interplay between our 'overtones' and the external driver. In any case a full understanding of the destabilizing mechanism associated to very narrow distributions of resistance times requires further investigation.

This research has received funding from the European Research Council under the European Union's Seventh Framework Programme (FP/2007 2013)/ERC Grant Agreement n. 740704.

Author contribution statement

G.G.J. carried out the simulations and created the figures. All authors discussed the results and contributed equally to writing the manuscript. All authors read and approved the final manuscript.

References

1. W.O. Kermack, A.G. McKendrick, in *Proceedings of the Royal Society of London A: Mathematical, Physical and Engineering Sciences* (The Royal Society, 1927), Vol. 115, pp. 700–721
2. R.M. Anderson, R.M. May, B. Anderson, in *Infectious diseases of humans: dynamics and control* (Wiley Online Library, 1992), Vol. 28
3. H.W. Hethcote, SIAM Rev. **42**, 599 (2000)
4. A. Korobeinikov, G.C. Wake, Appl. Math. Lett. **15**, 955 (2002)
5. K.L. Cooke, J.L. Kaplan, Math. Biosci. **31**, 87 (1976)
6. H.W. Hethcote, Bull. Math. Biol. **35**, 607 (1973)
7. R. Xu, Z. Ma, Chaos, Solitons Fract. **41**, 2319 (2009)
8. A.S. Klovdahl, Soc. Sci. Med. **21**, 1203 (1985)
9. S. Eubank, H. Guclu, V.A. Kumar, M.V. Marathe, A. Srinivasan, Z. Toroczkai, N. Wang, Nature **429**, 180 (2004)
10. M.E. Newman, Phys. Rev. E **66**, 016128 (2002)
11. V. Colizza, A. Barrat, M. Barthélemy, A. Vespignani, Proc. Natl. Acad. Sci. USA **103**, 2015 (2006)
12. S. Risau-Gusman, G. Abramson, Eur. Phys. J. B **60**, 515 (2007)
13. J.P. Aparicio, H.G. Solari, Math. Biosci. **169**, 15 (2001)
14. H.W. Hethcote, M.A. Lewis, P. Van Den Driessche, J. Math. Biol. **27**, 49 (1989)
15. T. Zhang, Z. Teng, Nonlinear Anal. Real World Appl. **9**, 1409 (2008)
16. L. Wen, X. Yang, Chaos Solitons Fract. **38**, 221 (2008)
17. T. Zhang, J. Liu, Z. Teng, Appl. Math. Comput. **214**, 624 (2009)
18. Y. Enatsu, Y. Nakata, Y. Muroya, Acta Math. Sci. **32**, 851 (2012)
19. H.W. Hethcote, H.W. Stech, P. Van Den Driessche, SIAM J. Appl. Math. **40**, 1 (1981)
20. S. Gonçalves, G. Abramson, M.F. Gomes, Eur. Phys. J. B **81**, 363 (2011)
21. K.L. Cooke, P. Van Den Driessche, J. Math. Biol. **35**, 240 (1996)
22. D.T. Gillespie, J. Phys. Chem. **81**, 2340 (1977)
23. H.W. Hethcote, Math. Biosci. **28**, 335 (1976)
24. H. Stech, M. Williams, J. Math. Biol. **11**, 95 (1981)
25. F. Rozenblit, M. Copelli, J. Stat. Mech. Theory Exp. **2011**, P01012 (2011)
26. G. Abramson, S. Gonçalves, M.F. Gomes, arXiv:1303.3779 (2013)